

"A Thermodynamic Study of Nonstoichiometric
Cerium Dioxide"*

THIS DOCUMENT CONFIRMED AS
UNCLASSIFIED

DIVISION OF CLASSIFICATION

BY Jack H. Kahn/wier

DATE 11/6/72

R. J. Panlener** and R. N. Blumenthal

Metallurgy and Materials Science, College of Engineering
Marquette University, Milwaukee, Wisconsin 53233

ABSTRACT

Thermogravimetric measurements were performed on nonstoichiometric CeO_{2-x} in the temperature range 700° to $1500^{\circ}C$ and from oxygen pressures of 10^{-1} to 10^{-26} atm. From this data the deviation from stoichiometry $x = x(T, P_{O_2})$ was determined. The thermodynamic quantities $\Delta\bar{H}_{O_2}$ and $\Delta\bar{S}_{O_2}$ were calculated in the region $0.0003 \leq x \leq 0.3$ and found to be independent of temperature.

In the composition region $x < 0.001$, the thermogravimetric data is assumed to be influenced by impurities.

In the region $0.001 < x < 0.01$, the variation of $\Delta\bar{S}_{O_2}$ with x is consistent with a defect model involving randomly distributed doubly ionized oxygen vacancies. The experimental $P_{O_2}^{-1/5}$ dependence of x is rationalized on the basis of the above model and the observation that $\Delta\bar{H}_{O_2}$ (≈ 9.8 eV) exhibits a slight dependence on x . It is postulated that the variation in $\Delta\bar{H}_{O_2}$ results from an increase in the lattice parameter with x .

* Supported by the U.S. Atomic Energy Commission. This is AEC report COO-1441-18.

**This paper is based in part on a thesis submitted by R. J. Panlener in partial fulfillment of the requirements for the Ph.D. degree, Marquette University, August 1972.

MASTER

DISCLAIMER

This report was prepared as an account of work sponsored by an agency of the United States Government. Neither the United States Government nor any agency Thereof, nor any of their employees, makes any warranty, express or implied, or assumes any legal liability or responsibility for the accuracy, completeness, or usefulness of any information, apparatus, product, or process disclosed, or represents that its use would not infringe privately owned rights. Reference herein to any specific commercial product, process, or service by trade name, trademark, manufacturer, or otherwise does not necessarily constitute or imply its endorsement, recommendation, or favoring by the United States Government or any agency thereof. The views and opinions of authors expressed herein do not necessarily state or reflect those of the United States Government or any agency thereof.

DISCLAIMER

Portions of this document may be illegible in electronic image products. Images are produced from the best available original document.

In the composition region $0.01 < x < 0.1$, $x \propto P_{O_2}^{-1/n}$ with $1 < n < 5$, and in the region $0.3 > x > 0.1$, $x \propto P_{O_2}^{-1/n}$ with n increasing rapidly with x to $n \approx 30$. This behavior is believed to be a manifestation of increasing defect interaction with increasing departures from stoichiometry. It is interesting to note that the ordered phase observed by Bevan and Kordis between $CeO_{1.72}$ and $CeO_{1.70}$ was not observed in this study at temperatures between 1300° and $1500^\circ C$.

INTRODUCTION

Nonstoichiometric cerium dioxide, CeO_{2-x} , is a metal excess n-type semiconductor based on several experimental investigations.¹⁻¹⁰ Previous thermodynamic investigations¹⁻⁴ of CeO_{2-x} have been conducted primarily for the purpose of studying the phase relationships in the Ce_2O_3 - CeO_2 system, with little emphasis regarding the nonstoichiometric defect structure. For this reason, thermodynamic information for compositions quite close to stoichiometry, i.e., $x < 10^{-2}$ in CeO_{2-x} , is lacking in the literature. Alternatively, several electrical conductivity investigations⁵⁻¹⁰ have been performed at temperatures and oxygen pressures corresponding to $x < 10^{-2}$. Unfortunately, the nature of the nonstoichiometric defect structure inferred from these studies is not in unanimous agreement. Therefore, the purpose of this paper is to report the results of our thermogravimetric measurements extended to $x \approx 10^{-4}$, and to use these results to clarify the interpretation of the nonstoichiometric defect structure.

The fact that the α fluorite phase has an extremely large homogeneity range at high temperatures has been clearly established. X-ray measurements by Brauer and Glingerich^{2,11} indicated a single phase region exists between CeO_2 and $\text{CeO}_{1.78}$, with a miscibility gap occurring at temperatures below 685°C. Their oxygen dissociation measurements between 600° and 1050°C indicate a single phase region extending to $\text{CeO}_{1.81}$ above 700°C, and to $\text{CeO}_{1.67}$ above 800°C. Similar phase relationships were found by Kuznetsov et al.³ with galvanic cell and gas equilibrium measurements. Oxygen dissociation measurements between 636° and 1169°C by Bevan and Kordis⁴ indicate a single phase region from CeO_2 to $\text{CeO}_{1.72}$ above 685°C.

To account for the nonstoichiometric behavior observed at large departures from stoichiometry, Kofstad and Hed¹² have proposed a defect model involving singly and doubly ionized cerium interstitials and local-

ized electrons. Conversely, Atlas¹³ has proposed a statistical model involving partial ordering of singly ionized oxygen vacancies and localized electrons.

In addition to the thermodynamic studies, several electrical conductivity studies have been performed on CeO_{2-x} . Greener et al.⁶ measured the electrical conductivity from 650° to 1400° C and from 1 to 0.006 atm of oxygen and they suggest the nonstoichiometric defects are either quadruply ionized cerium interstitials or fully ionized oxygen vacancy pairs. Kevane¹⁴, however, concluded the data of Greener et al. coupled with that of Bevan and Kordis⁴ is not inconsistent with an oxygen vacancy model incorporating multiple states of ionization.

Blumenthal and Laubach⁹ measured the electrical conductivity from 800° to 1500° C and from 1 to 10^{-17} atm of oxygen and showed the results to be consistent with an oxygen vacancy model involving multiple states of ionization. Blumenthal et al.¹⁰, however, point out several difficulties with this interpretation and, with the electrical conductivity measurements extended to 10^{-21} atm of oxygen, conclude the behavior is more likely represented by a defect model involving cerium interstitials in multiple states of ionization.

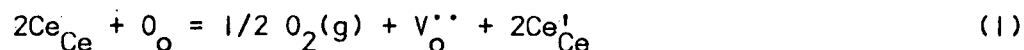
A serious difficulty with defect structure analysis of electrical conductivity data is the presence of electron mobility, which may exhibit both temperature and compositional dependence. In addition, these analyses have assumed the law of mass action to be valid, while no means are available to actually test the mass action assumptions. These problems, however, are avoided in an analysis of thermodynamic data.

Recently, Steele and Floyd¹⁵ have measured the oxygen self-diffusion in CeO_{2-x} from 850° to 1150° C. Their results provide convincing evidence that the predominant nonstoichiometric defects are oxygen vacancies. How-

ever, their measurements were not sensitive to either the state of aggregation of the defects (i.e., whether the defects are paired or not) or the state of ionization. These questions are clarified in this study.

THEORY

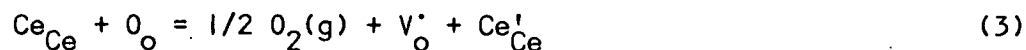
According to the diffusion study of Steele and Floyd,¹⁵ the nonstoichiometric defects in CeO_{2-x} are in all probability oxygen vacancies. If the oxygen vacancies are doubly ionized, the following defect reaction may be written:



where, according to Kröger's¹⁶ notation, Ce_{Ce} and O_{O} are normal Ce and O ions on their respective sites, $\text{V}_{\text{O}}^{\bullet\bullet}$ is a doubly ionized oxygen vacancy, and Ce_{Ce}' is an electron localized on a Ce ion. The electrons are assumed localized in CeO_{2-x} since the electronic conduction process is a "hopping type" process.¹⁷ Applying the law of mass action to the defect reaction in Eq. (1) yields

$$\sigma \propto x \propto P_{\text{O}_2}^{-1/6} \quad (2)$$

where σ is the electronic conductivity, x the deviation from stoichiometry, and P_{O_2} the partial pressure of oxygen. If the oxygen vacancies in CeO_{2-x} are singly ionized, the defect reaction may be written as



and the law of mass action predicts

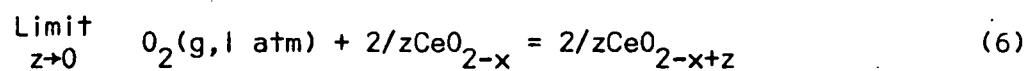
$$\sigma \propto x \propto P_{\text{O}_2}^{-1/4} \quad (4)$$

However, what is observed experimentally is that the electrical conductivity over a significant range of temperatures and oxygen pressures exhibits a

$$\sigma \propto P_{\text{O}_2}^{-1/5} \quad (5)$$

dependence.^{6,9,10} In order to rationalize the $P_{O_2}^{-1/5}$ dependence, several different defect structures have been proposed including 1) a combination of singly and doubly ionized oxygen vacancies,^{9,14} 2) quadruply ionized oxygen divacancies,⁶ and 3) quadruply ionized cerium interstitials.^{6,10} The interstitial interpretation, however, is not consistent with the recent diffusion study.¹⁵ The oxygen divacancy, alternatively, is difficult to rationalize on physical grounds based on a coulombic repulsion argument. And finally, Blumenthal and Hofmaier,²⁵ from a combination of constant composition electrical conductivity and thermogravimetric data, suggest that the state of ionization of the nonstoichiometric defects is not changing over a wide range of composition. This, however, is not consistent with a defect model involving multiple states of ionization. Thus it appears that the defect models for CeO_{2-x} based on the law of mass action have not been successful in rationalizing the observed P_{O_2} dependence of electrical conductivity measurements. This suggests that the law of mass action may not be entirely valid for CeO_{2-x} .

The assumptions inherent in the mass action approach may be tested by obtaining the relative partial molal enthalpy, $\Delta\bar{H}_{O_2}$, and entropy, $\Delta\bar{S}_{O_2}$, and comparing the compositional dependencies of these quantities with that predicted for dilute solution behavior. The relative partial molal quantities for CeO_{2-x} are defined as the changes in the thermodynamic quantities accompanying the reaction



These quantities for oxygen in CeO_{2-x} may be calculated from the following well known relations:

$$\Delta\bar{G}_{\text{O}_2} = \Delta\bar{H}_{\text{O}_2} - T\Delta\bar{S}_{\text{O}_2} \quad (7)$$

$$\Delta\bar{G}_{\text{O}_2} = RT \ln P_{\text{O}_2} \quad (8)$$

$$\Delta\bar{H}_{\text{O}_2} = - \left[\frac{\partial(\Delta\bar{G}_{\text{O}_2}/T)}{\partial(1/T)} \right]_{x = \text{constant}} \quad (9)$$

The compositional dependencies of $\Delta\bar{H}_{\text{O}_2}$ and $\Delta\bar{S}_{\text{O}_2}$ serve as a criterion for the overall validity of the law of mass action. If $\Delta\bar{H}_{\text{O}_2}$ is composition independent, and if $\Delta\bar{S}_{\text{O}_2}$ varies in a fashion consistent with a random entropy of mixing model, the solution behavior is then referred to as "dilute", and is consistent with the law of mass action. However, if $\Delta\bar{H}_{\text{O}_2}$ varies with composition, either the nonstoichiometric defect structure is changing, or, some type of defect interaction is occurring. If the former is true, the law of mass action may be applied with additional considerations. If the latter is true, the law of mass action is not valid, and $\Delta\bar{S}_{\text{O}_2}$ will deviate from a random entropy model, with the extent of the deviation depending upon the nature of the defect interaction.

If the defect species are randomly distributed, the quantity $\Delta\bar{S}_{\text{O}_2}$ will exhibit specific compositional dependencies, depending upon the defect structure. For example, the entropy change for the defect reaction in Eq. (1) may be expressed by

$$\Delta S = \bar{S}_{\text{V}_0} + 2\bar{S}_{\text{Ce}'_{\text{Ce}}} + 1/2 S_{\text{O}_2}^{\circ} - 2\bar{S}_{\text{Ce}_{\text{Ce}}} - \bar{S}_{\text{O}_0} \quad (10)$$

where

$$\Delta \bar{S}_{O_2} = -2\Delta S \quad (11)$$

The quantity $S_{O_2}^O$ is ≈ 60 entropy units in the temperature range of this investigation. The partial molal terms, \bar{S}_i , may be divided into vibrational, S_i^V , and configurational, S_i^C , terms. If the defects are randomly distributed,

$$S_i^C = -R \ln X_i \quad (12)$$

where X_i is the site fraction of species i . For this case,

$$\begin{aligned} \Delta S = & 1/2 S_{O_2}^O + S_{V_0}^V + 2(S_{Ce_{Ce}^V} - S_{Ce_{Ce}^V}) - S_{O_0}^V - R \ln[V_0^{**}] \\ & - 2R \ln[Ce_{Ce}^{\cdot}] + R \ln[Ce_{Ce}] + R \ln[O_0] \end{aligned} \quad (13)$$

where the square brackets refer to site fractions. For small departures from stoichiometry, the last two terms in Eq. (13) are negligible. Using the relations

$$[Ce_{Ce}^{\cdot}] = 2[V_0^{**}] \quad (14)$$

$$x/2 = [V_0^{**}] \quad (15)$$

ΔS may be written

$$\Delta S = 1/2 S_{O_2}^O + \Delta S_+^V - 3R \ln x + 2R \ln 2 \quad (16)$$

where ΔS_+^V is the total vibrational entropy change. Combining Eqs. (11) and (16),

$$-\Delta \bar{S}_{O_2} = 2\Delta S = S_{O_2}^O + 2\Delta S_+^V - 6R \ln x + 4R \ln 2 \quad (17)$$

If the vibrational terms are independent of composition, the compositional dependence of $\Delta\bar{S}_{O_2}$ may be expressed by

$$\partial\Delta\bar{S}_{O_2}/\partial\ln x = 6R \quad (18)$$

Similar arguments may be used to obtain the compositional dependence of $\Delta\bar{S}_{O_2}$ for other defect reactions. For randomly distributed oxygen vacancies, the general expression is

$$\partial\Delta\bar{S}_{O_2}/\partial\ln x = 2(n+1)R \quad (19)$$

where n represents the state of ionization of the oxygen vacancy. Similarly for cerium interstitials or oxygen divacancies,

$$\partial\Delta\bar{S}_{O_2}/\partial\ln x = (n+1)R \quad (20)$$

where n represents the state of ionization of the defect.

When $\Delta\bar{S}_{O_2}$ varies in a manner other than that described above, it may be a result of a changing defect structure. In this case, the compositional dependence of $\Delta\bar{S}_{O_2}$ may be related to a weighed average of the appropriate ΔS models. However, when the deviation from the "random" compositional dependence is due to defect interaction, the above treatments are not valid; and $\Delta\bar{S}_{O_2}$ may only be interpreted with more rigorous statistical mechanical treatments.

EXPERIMENTAL

The experimental objective of this work was to determine the equilibrium deviation from stoichiometry in "pure" CeO_2 as a function of temperature and oxygen partial pressure. A thermogravimetric technique employing a microbalance was used to measure the changes in weight experienced by a sample of CeO_2 as the external variables of temperature and oxygen partial pressure were changed relative to a reference thermodynamic state¹⁸.

Sintered samples were prepared from American Potash & Chemical Corporation CeO_2 powder having designated purities* of 99.99% (4N CeO_2) and 99.999% (5N CeO_2) respectively. The preparation techniques employed were similar to those used in a previous study⁹. Samples were shaped in the form of parallelepipeds weighing approximately 0.5 gm, with the surfaces polished and all edges smoothed to minimize the possibility of material loss due to sample strain and cracking. Grooves were ground on two opposing sample sides with a silicon carbide disk to allow the samples to fit securely into a J-shaped sample holder constructed of short pieces of rod fused together. Table I contains the results of mass spectrographic analyses for the 4N CeO_2 powder and a typical sintered sample prepared from 5N CeO_2 powder.

*Purity designations are with respect to rare earth impurities only.

A Cahn R.G. Electrobalance was used to measure the weight changes of a CeO_2 sample suspended with 4 mil Pt/Pt - 40% Rh wire and short lengths of 10 mil ruby rod in a high temperature furnace. Floor mounting pads of high damping capacity glass-filled epoxy-resin were used to isolate the balance from mechanical vibrations. With this arrangement the overall noise level was $\pm 1 \mu\text{g}$. The balance output was measured with a Doric integrating Microvoltmeter which (1) permitted the use of the maximum filtering available on the balance, and (2) obviated the use of the "Mass Dial" (zero-offset) on the Cahn balance.

Temperatures from 700°C - 1500°C were obtained with a Mo wound resistance furnace, measured with reference grade Pt-Pt/13% Rh thermocouples, and controlled to approximately $\pm 1/2^\circ\text{C}$ with a Barber-Colman model 477 Capacital, and a model 621 Power controller. Controlled oxygen partial pressures from 10^{-1} to 10^{-26} atm were obtained from premixed and analyzed O_2 -Ar and CO - CO_2 mixtures. Linear gas velocities ranged from 2.5 to 4.0 cm/sec, which is greater than the 0.9 cm/sec value recommended by Darken and Gurry¹⁹ to eliminate thermal separation effects.

The thermogravimetric system was operated at a reduced total pressure of 0.1 atm to reduce the effect of gas convection and to minimize the effect of buoyancy²⁰. The reduced pressures were obtained with a high capacity (5 liter/min) Kinney vacuum pump, controlled to ± 1 mm Hg with a Gilmont Cartesian diver-type pressure Controller, and measured with a Gilmont Positive Closed End Manometric Gage.

Spurious weight changes¹⁸, not attributable to the sample, were observed as the total system pressure was varied. These weight changes were believed to be the result of thermomolecular flow (TMF) of gases^{21,22}. The influence of the total system pressure, temperature, and gas species on

this phenomenon was investigated. Under isothermal conditions, negligible error was introduced when the total pressure was controlled at 0.1 atm¹⁸. In addition, it was found that changing gas species under isothermal and isobaric conditions led to measurable TMF weight changes. Therefore, an inert sample of Al₂O₃ was prepared to closely approximate the physical shape of the CeO₂ samples. The effect of changing gases was observed in exactly the same manner and at all temperatures as the actual weight change measurements were made. These values were then used to correct all measured weight changes.

The experimental procedure adopted in this study, based on considerations of the various system problems and behavior, was to measure all weight changes isothermally relative to the thermodynamic state of (T, P_{O₂} = 0.1 atm). It was particularly important that the determination of the individual weight changes occurred over the shortest possible time periods, thus avoiding errors due to balance drift and local disturbances. Since the oxidation rates of CeO₂ are extremely high, the relative weight measurements were made from the reduced to the oxidized state. In addition, all measurements were made statically, thus avoiding problems associated with the forces arising from the flow of gases.

The experimental precision for small weight changes was found to be $\pm 2-3 \mu\text{g}$, based on the ability to reproduce an absolute sample weight. This reproducibility was tested with CeO₂ samples, with inert samples, with the same gas species, and with different gas species. In all cases, the technique used was identical to that used for the actual measurements. The precision for large weight changes was found to be $\pm 0.2-0.3\%$ ¹⁸.

It is interesting to note that 1400° and 1500° C, some problems of sample volatilization and material condensation occurred, but did not seriously limit the accuracy of these measurements.

RESULTS AND DISCUSSION

The results of the thermogravimetric measurements on CeO_{2-x} are shown in Fig. 1, where isotherms of $\log \Delta W/W$ are plotted as a function of $\log P_{\text{O}_2}$ from 700° to 1500°C, and from 10^{-2} to 10^{-26} atm of oxygen. The individual data points represent average values for four samples, three prepared from $5\text{N}\text{CeO}_2$ powder and one from $4\text{N}\text{CeO}_2$ powder. In general, no differences in behavior were observed between these samples¹⁸. The error bars for small weight changes are illustrated in the lower right hand corner of Fig. 1. The precision for the larger weight changes may be adequately represented by the size of the data points.

The deviation from stoichiometry in CeO_{2-x} , may be calculated from the weight change data provided the measurements are made relative to a reference state of known composition. If the reference state is stoichiometric CeO_2 , then

$$x = \frac{\Delta W}{W} \frac{AW_{\text{O}}}{MW_{\text{CeO}_2}} \quad (21)$$

where ΔW is the relative weight change, W the sample weight, AW_{O} the atomic weight of oxygen, and MW_{CeO_2} the molecular weight of CeO_2 .

Eq. (21) is valid when

$$x(T, P_{\text{O}_2}) \gg x(T, P_{\text{O}_2} = 0.1 \text{ atm})$$

where $x(T, P_{\text{O}_2} = 0.1 \text{ atm})$ is the reference state used in this investigation. For the measurements at or below 1000°C in Fig. 1, the above condition is fulfilled, and the deviation from stoichiometry may be obtained using Eq. (21). For all measurements above 1000°C, however, the condition is not fulfilled, and significant sample weight losses occur with increasing temperature from 1000° to 1500°C in O_2 at 0.1 atm. Therefore, to determine the deviation from stoichiometry from this data, corrections for the non-

stoichiometry in the reference state are necessary.

Several attempts were made to estimate the reference state nonstoichiometry, and the results are compared in Fig. 2, where the estimated values of $\log \Delta W/W$ for ($T, P_{O_2} = 0.1 \text{ atm}$) relative to CeO_2 are plotted versus $1/T$. These values were obtained by the following methods:

1. Evaluating the tangents to the $1000^\circ - 1300^\circ\text{C}$ isotherms in Fig. 1 at $P_{O_2} \sim 10^{-5}$, and then extrapolating the tangents to 0.1 atm. The electrical conductivity of CeO_{2-x} in this temperature and pressure region behaves in a similar manner; i.e., the $\log \sigma - \log P_{O_2}$ slopes are constant between 10^{-5} and 0.1 atm.¹⁰

2. Measuring $\Delta W/W$ on cooling from 1500°C to below 1000°C in O_2 at 0.1 atm for both a CeO_2 sample and an identically shaped Al_2O_3 sample. These values are considered reasonably accurate at the higher temperatures, while those at the lower temperatures are questionable due to experimental problems.

3. Determining the constants necessary to be added to a given $\Delta W/W$ isotherm such that the $\log \Delta W/W - \log P_{O_2}$ and the $\log \sigma - \log P_{O_2}$ slopes are equal for that isotherm. These values may be high if the mobility exhibits any compositional dependence, or if multiple states of ionization are present.

4. Calculating the $\Delta W/W$ values at 0.1 atm from a model based on the lower temperature behavior coupled with observations of the electrical conductivity behavior. In the region from 700° to 1100°C , and from $\log \Delta W/W$ between -4.00 and -3.60,

$$\Delta W/W \propto P_{O_2}^{-1/5}$$

The electrical conductivity exhibits a similar $P_{O_2}^{-1/5}$ dependence in the corresponding regions of temperature and P_{O_2} , and also at higher temperatures at $P_{O_2} \sim 0.1 \text{ atm}$ ¹⁰. Therefore, in an empirical manner, the $\Delta W/W$ corrections were obtained from the relations

$$K = (\Delta W/W)^5 P_{O_2} \quad (22)$$

and

$$K = K_0 \exp(-\Delta H/kT) \quad (23)$$

where values for K_0 and ΔH were obtained from the lower temperature $\Delta W/W$ data. (A value of 9.7 eV was used for ΔH .) This calculation assumes the $P_{O_2}^{-1/5}$ dependence to be valid at high temperatures, and assumes that $\Delta W/W$ varies in a simple exponential manner at 0.1 atm, which is essentially what is observed for the electrical conductivity¹⁰.

Evaluation of the four methods indicates that (4) represents a reasonable compromise, and is possibly the most accurate. Therefore, the $\Delta W/W(T, P_{O_2})$ data was corrected for the nonstoichiometry in the reference state by adding values of $\Delta W/W(T, P_{O_2} = 0.1 \text{ atm})$ calculated from Eqs. (22) and (23). The tolerance of the corrections was estimated to be $\pm 20\%$ or better.

The deviation from stoichiometry calculated from the corrected thermogravimetric data is shown in Fig. 3, where isotherms of $\log x$ in CeO_{2-x} are plotted versus $\log P_{O_2}$ from 700°C to 1500°C, and from 10^{-1} to 10^{-26} atm of oxygen. The error bars about the values of $\log x$ at 0.1 atm represent the estimated 20% tolerance of the $\Delta W/W$ corrections. Discussion of the nonstoichiometric behavior may be directed toward four different regions of composition.

In the region $\log x < -3.0$, the behavior is presumably influenced by impurities. The electrical conductivity of sintered specimens prepared from identical $5N CeO_2$ powder was found to be impurity controlled at these temperatures and oxygen pressures¹⁰. Also, the mass spectrographic analyses presented in Table I show that the concentrations of several

Impurities are on the order of the nonstoichiometric defect concentrations in this composition region. In addition to the purity problem, the the data in this region exhibits large uncertainties because the weight changes are not large compared to the thermogravimetric system tolerance, as illustrated by the error bars in Fig. 1.

In the region $-2.0 < \log x < -2.4$, the data is best characterized by

$$x \propto P_{O_2}^{-1/5}$$

It should be noted that the electrical conductivity is reported¹⁰ to exhibit a similar pressure dependence at these temperatures and oxygen pressures.

In the region $-2.4 < \log x < -1.2$, the data may be characterized by an expression of the type

$$x \propto P_{O_2}^{-1/n}$$

where n varies from 5 to less than 1 at 700°C, while at higher temperatures the variation from $n = 5$ is substantially less.

And in the region $\log x < -1.2$, the observed P_{O_2} dependence of x decreases rapidly with increasing x , with $x \propto P_{O_2}^{-1/n}$ where $n \approx 30$ at the highest temperatures. In this region, Bevan and Kordis have observed a high temperature phase between $CeO_{1.72}$ and $CeO_{1.70}$ ($-\log x = 0.55$ to 0.52) extending to temperatures as high as to 1170°C. However in this study at temperatures between 1300° and 1500°C, this phase was not observed. This result is consistent with the hypothesis of an ordered phase, and this behavior is similar to the behavior of other ordered phases occurring at low temperatures in CeO_{2-x} ²³.

The thermodynamic quantities $\Delta\bar{H}_{O_2}$ and $\Delta\bar{S}_{O_2}$ may be calculated from the data in Fig. 3 using Eqs. (7) - (9). Fig. 4 is a plot of $\log P_{O_2}$

versus $1/T$ where the $\log P_{O_2}$ - temperature values for the constant compositions noted in the figure were obtained from the isothermal lines in Fig. 3. The least squares lines in Fig. 4 were determined for the individual compositions using all data below the approximate P_{O_2} value of 10^{-7} , and have been extrapolated to the higher P_{O_2} values. The values above 10^{-7} correspond to those possibly affected by the uncertainty in the reference state stoichiometry correction.

The significant features in Fig. 4 are:

1. For constant composition $\log P_{O_2}$ varies linearly with $1/T$ for all temperatures and at all compositions, while the slopes differ for the different compositions. The linear behavior indicates $\Delta\bar{H}_{O_2}$ and $\Delta\bar{S}_{O_2}$ are independent of temperature. However, the different slopes indicate the quantities will exhibit some compositional dependence.

2. The data above $P_{O_2} = 10^{-7}$ shows very little deviation from the extended least square lines, indicating that the reference state stoichiometry corrections are in all probability quite accurate, and the $\pm 20\%$ tolerance is most likely an overestimate of the error.

For the purpose of a comparison with the results of Bevan and Kordis⁴, the quantities $\Delta\bar{H}_{O_2}$ and $\Delta\bar{S}_{O_2}$ are plotted versus x in Figs. 5 and 6. As illustrated in these figures, the agreement with Bevan and Kordis is excellent for x less than approximately 0.15. However, for larger x the behavior is different. A possible reason for this discrepancy is that Bevan and Kordis determined their values from thermogravimetric data taken over the temperature range 636°C to 1169°C. The values from this study were determined from data at appreciably higher temperatures. Thus it appears that at large departures from stoichiometry, $\Delta\bar{H}_{O_2}$ and $\Delta\bar{S}_{O_2}$ may not be temperature independent as initially interpreted. This conclusion is consistent with the observation that the ordered phase $CeO_{1.72-1.70}$ disappears at higher temperatures.

Although important for comparison, the results shown in Figs. 5 and 6 do not significantly reflect the emphasis of this investigation, which was to focus on the nonstoichiometric behavior in regions close to stoichiometry. Therefore, in Figs. 7 and 8, $\Delta\bar{H}_{O_2}$ and $\Delta\bar{S}_{O_2}$ are plotted versus $\log x$. These plots illustrate the behavior in the region closer to stoichiometry, and essentially parallel the deviation from stoichiometry data shown in Fig. 3. Discussion of the $\Delta\bar{H}_{O_2}$ and $\Delta\bar{S}_{O_2}$ behavior is directed toward three different regions of composition.

In the region $\log x < -3.0$, the quantities $\Delta\bar{H}_{O_2}$ and $\Delta\bar{S}_{O_2}$ are assumed to be influenced by impurities, as was the thermogravimetric data in this composition region.

In the region $-3.0 < \log x < -2.0$, both $\Delta\bar{H}_{O_2}$ in Fig. 7, and $\Delta\bar{S}_{O_2}$ in Fig. 8 are found to vary linearly with $\log x$. The variation in $\Delta\bar{H}_{O_2}$ indicates that the $P_{O_2}^{-1/5}$ dependence of x observed in this region in Fig. 3 cannot be interpreted on the basis of a mass action defect model involving a single state of ionization. Rather, the variation of $\Delta\bar{H}_{O_2}$ with x is consistent with a change in defect structure and/or defect interaction.

The linear variation in $\Delta\bar{S}_{O_2}$, alternatively, is consistent with a randomly distributed defect model. It is observed that the compositional dependence of $\Delta\bar{S}_{O_2}$ for the doubly ionized vacancy model,

$$\partial\Delta\bar{S}_{O_2} / \partial \ln x = 6R \quad (18)$$

provides an excellent representation of the experimental data. This is illustrated by comparing the slope of the line calculated from Eq. (18) with the actual data as shown in Fig. 8. Thus, in this composition region, it appears that $\Delta\bar{S}_{O_2}$ is consistent with random distribution of defects, although $\Delta\bar{H}_{O_2}$ exhibits a slight dependence on composition.

If the variation in $\Delta\bar{H}_{O_2}$ is the result of slight "defect-defect" interactions, the random configurational entropy model is only an approximation. Whereas, if the variation in $\Delta\bar{H}_{O_2}$ is the result of a varying "defect-host lattice" interaction, the random configurational entropy model is valid. Sims²⁴ observed a small linear lattice parameter increase with composition close to stoichiometry at high temperatures. If this lattice parameter increase is due to the electronic defects (Ce_{Ce}^{\cdot}) for example, a model incorporating a varying $\Delta\bar{H}_{O_2}$ and random $\Delta\bar{S}_{O_2}$ is not unreasonable. The lattice parameter increase may affect $\Delta\bar{H}_{O_2}$, but have only a slight perturbation on the vibrational entropy.

As described below, this model may also be used to explain the $P_{O_2}^{-1/5}$ dependence of x observed in the composition region $-3.0 < \log x < -2.4$. The thermogravimetric data was calculated using the values of $\Delta\bar{H}_{O_2}$ and assuming a random distribution of the doubly ionized oxygen vacancies. The equations used were

$$K = x^6 P_{O_2} \quad (24)$$

and

$$K = K_0 \exp(\Delta\bar{H}_{O_2}/kT) \quad (25)$$

where Eq. (24) is the mass action expression for doubly ionized oxygen vacancies. The $x^6 P_{O_2}$ term represents the random configurational entropy. Eq. (25) is similar to the mass action expression

$$K \propto \exp(\Delta S^\circ/k) \exp(-\Delta H^\circ/kT) \quad (26)$$

However, in Eq. (25), $\Delta\bar{H}_{O_2}$ will vary with composition, whereas in the mass action treatments, ΔH° is constant. The results of this calculation are shown in Fig. 9, where the constant K_0 was evaluated from the thermogravimetric data at $\log x = -3.00$ for each temperature. (As a test for consist-

ency, the results have been extended past $\log x = -2.00$ by accounting for the difference between $\Delta\bar{S}_{O_2}$ and the random distribution model for the $V_{O^{\bullet\bullet}}$ model in Fig. 8. However, no physical significance should be attributed to the results other than those for the region $-3.0 \leq \log x \leq 2.0$.) This calculation clearly demonstrates that the $P_{O_2}^{-1/5}$ dependence of x is consistent with a defect model of doubly ionized oxygen vacancies, provided $\Delta\bar{H}_{O_2}$ varies slightly with composition. This conclusion applies to the electrical conductivity data as well, thus rationalizing the $P_{O_2}^{-1/5}$ dependence of σ with the more plausible oxygen vacancy defect model.

In the region $\log x > -2.0$, $\Delta\bar{S}_{O_2}$ deviates from linear dependence on $\log x$, and $\Delta\bar{H}_{O_2}$ exhibits a minimum. This behavior is interpreted as due to an increase in the defect-host interaction, and undoubtedly the onset of defect-defect interaction. Blumenthal and Hofmaier²⁵ have concluded that the relation between x and the electron carrier concentration,

$$[Ce_{Ce}^{\bullet}] \propto x$$

remains unaltered over the composition range $-3.0 < \log x < -0.7$. This suggests that the nonstoichiometric defects are doubly ionized oxygen vacancies over entire nonstoichiometric composition region.

BIBLIOGRAPHY

1. Brauer, G., Gingerich, K. A. and Holtschmidt, U., J. Inorg. Nucl. Chem., 16, 77 (1960).
2. Brauer, G. and Gingerich, K. A., Rare Earth Research, ed. Kleber, E. G., New York: Macmillan Co., (1961).
3. Kuznetsov, F. A., Belyi, V. I. and Rezukhina, T. N., Dokl. Akad. Nauk, SSSR, 139, 1405 (1961).
4. Bevan, D. J. M. and Kordis, J., J. Inorg. Nucl. Chem., 26, 1509 (1964).
5. Rudolph, J., Z. Naturforsch., 14, 727 (1959).
6. Greener, E. H., Wimmer, J. M. and Hirthe, W. M., Rare Earth Research II, ed. Vorres, Karl S., New York: Gordon and Breach, 1964, p. 539.
7. Poluboyarinov, D. N., Shapiro, E. Ya., Bakunov, V. S., and Akopov, F. A., I.A. Nauk SSSR, N. Materialy, 2, 336 (1966).
8. Vinkurov, I. V., Zonn, Z. N. and Ioffe, V. A. Soviet Physics-Solid State, 9, 2659 (1968).
9. Blumenthal, R. N. and Laubach, J. E. Anisotropy in Single-Crystal Refractory Compounds, Ed. by W. Vahldiek and S. A. Mersol, New York: Plenum Press, 1968, pp. 138-150.
10. Blumenthal, R. N., Lee, P. W. and Panlener, R. J., J. Electrochem. Soc., 118, 123 (1971).
11. Brauer, G. and Gingerich, K. A., J. Inorg. Nucl. Chem., 16, 87 (1960).
12. Kofstad, P. and Hed, A. Z., J. Amer. Ceram. Soc., 50, 681 (1967).
13. Atlas, L. M., J. Phys. Chem. Solids, 29, 91 (1968).
14. Kevane, G. J., Phys. Rev., 133, 1431 (1964).
15. Steele, B. C. H. and Floyd, J. M., Proc. Brit., Cer. Soc., 19, 55 (1971).
16. Kroger, F. A., The Chemistry of Imperfect Crystals, New York: John Wiley and Son, 1964.
17. Blumenthal, R. N. and Panlener, R. J., J. Phys. Chem Solids, 31, 1190 (1970).

18. Panlener, R. J. "A Study of the Defect Structure of Pure and Calcia Doped Nonstoichiometric Cerium Dioxide," Ph.D. Dissertation Marquette University, Milwaukee, Wisconsin (1972).
19. Darken, L. S., and Gurry, R. W., Am. Chem. Soc. 67 (8), 1398 (1945).
20. Tripp, W. C., Vest, R. S., and Tallan, N. M. Vacuum Microbalance Tech., 4 141-157 (1965).
21. Vacuum Microbalance Techniques, Vol. I-VIII, Plenum Press, New York, 1961-1971.
22. Wolsky, S.P., and Zdanuk, E. J., Ed., Ultra Micro Weight Determination in Controlled Environments, Interscience, New York, 1969.
23. Bevan, D. J. M., J. Inorg. Nucl. Chem.; 1, 49 (1955).
24. Sims, J. R., Jr., personal Communication. (Ph.D. research in progress at Marquette University, Milwaukee, Wisconsin.)
25. Blumenthal, R. N. and Hofmaier, R. L., submitted to J. Electrochem. Soc.

Table 1

Mass Spectrographic Analysis of 4NCeO_2 Powder and a 5NCeO_2
Sintered Sample

<u>Element</u>	<u>4NCeO_2</u>	<u>5NCeO_2</u>	<u>Element</u>	<u>4NCeO_2</u>	<u>5NCeO_2</u>
Li	20	0.3	Ag	<0.4	≤0.2
Be	<0.002	<0.01	Cd	<0.07	<0.2
B	0.1	≤7.0	In	<0.02	<0.1
F	30	20.0	Sn	0.06	0.2
Na	300	15.0	Sb	<0.05	<0.2
Mg	10	2.0	Te	<0.1	<0.3
Al	30	15.0	I	<0.1	<0.1
Si	20	20.0	Cs	<0.02	<0.06
P	200	2.0	Ba	2	<1.0
S	100	7.0	La	1	<0.5
Cl	3	10.0	Pr	2	10.0
K	600	15.0	Nd	≤1	10.0
Ca	200	300.0	Sm	1	<1.0
Sc	<0.5	<0.1	Eu	1	10.0
Ti	20	2.0	Gd	≤4	<5.0
V	<0.01	≤0.03	Tb	1	2.0
Cr	1	0.2	Dy	2	1.0
Mn	0.1	0.2	Ho	0.6	≤0.3
Fe	10	6.0	Er	0.6	≤0.5
Co	<0.1	0.4	Tm	≤0.1	<0.1
Ni	≤0.2	20.0	Yb	1	≤1.0
Cu	0.6	0.2	Lu	<0.3	≤0.3
Zn	3	1.0	Hf	≤1	2.0
Ga(a)	-	-	Ta	<0.5	≤3.0
Ge	<0.3	<0.2	W	<0.2	<0.2
As	3	<0.02	Re	<0.1	<0.3
Se	≤0.2	<0.4	Os	<0.6	<1.0
Br	≤0.1	<0.3	Ir	<0.06	<0.2
Rb	0.5	<1.0	Pt	<0.2	<0.4
Sr	1	0.2	Au	<0.3	<0.4
Y	5	0.5	Hg	<0.3	<0.4
Zr	10	10.0	Tl	<0.1	<0.2
Nb	≤0.03	<0.02	Pb	10	1.0
Mo	≤0.06	<0.07	Bi	<0.1	<0.1
Ru	≤0.06	<0.1	Th	40	50.0
Rh	≤0.02	<0.02	U	<0.1	<0.06
Pd	<1	<0.2			

(a) Ce interference

LIST OF FIGURES

- Figure 1 Isothermal $\log \Delta W/W$ versus $\log P_{O_2}$ from 700° - 1500°C.
- Figure 2 Estimated reference state stoichiometry correction vs $1/T$ for 4 methods.
- Figure 3 Isothermal $\log x$ versus $\log P_{O_2}$ from 700° - 1500°C.
- Figure 4 $\log P_{O_2}$ vs $1/T$ for constant composition.
- Figure 5 $\Delta \bar{H}_{O_2}$ vs n in CeO_n .
- Figure 6 $\Delta \bar{S}_{O_2}$ vs n in CeO_n .
- Figure 7 $\Delta \bar{H}_{O_2}$ vs $\log x$ for CeO_{2-x} .
- Figure 8 $\Delta \bar{S}_{O_2}$ vs $\log x$ for CeO_{2-x} .
- Figure 9 Calculated values of $\log x - \log P_{O_2}$ for doubly ionized oxygen vacancy model.

